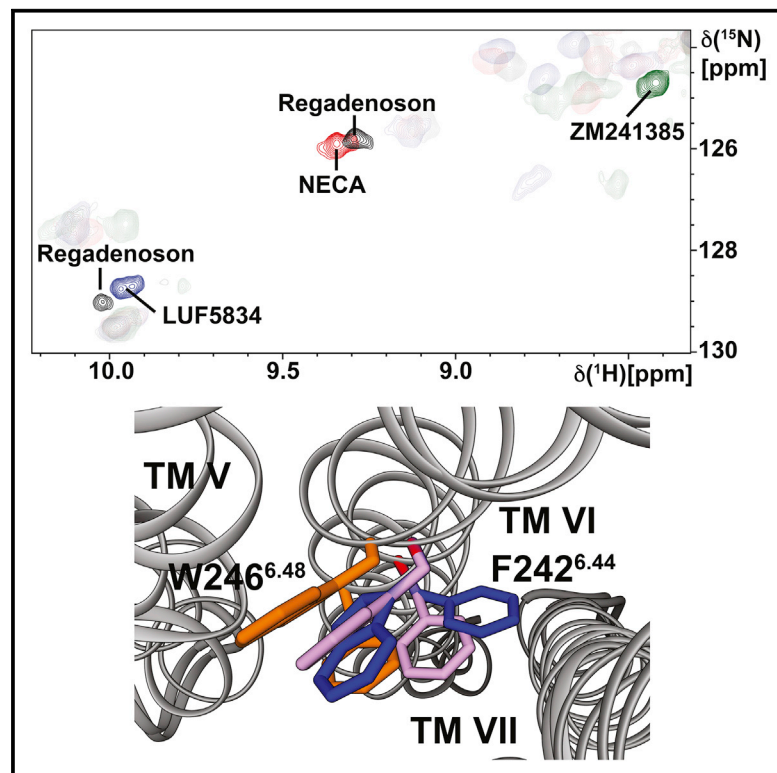


Structure

A_{2A} Adenosine Receptor Partial Agonism Related to Structural Rearrangements in an Activation Microswitch

Graphical Abstract



Authors

Matthew T. Eddy, Bryan T. Martin,
Kurt Wüthrich

Correspondence

matthew.eddy@ufl.edu

In Brief

New insight into the structural basis for partial activation of human GPCRs is presented. Using NMR spectroscopy in aqueous solution, Eddy et al. discovered that a highly conserved activation motif in A_{2A}AR complexes with partial agonists adopts a unique conformation, which differs from this motif in complexes with full agonists or antagonists.

Highlights

- NMR data reveal distinct activation motif conformations in partial agonist complexes
- Full and partial agonist complexes of A_{2A}AR share similar 3D polypeptide folds
- Partial and full agonism in a GPCR relates to different signal transduction pathways



Short Article

A_{2A} Adenosine Receptor Partial Agonism Related to Structural Rearrangements in an Activation Microswitch

Matthew T. Eddy,^{1,2,3,5,*} Bryan T. Martin,^{2,4} and Kurt Wüthrich¹¹Department of Integrative Structural and Computational Biology, The Scripps Research Institute, 10550 North Torrey Pines Road, La Jolla, CA 92037, USA²Departments of Biological Sciences and Chemistry, Bridge Institute, The University of Southern California, Los Angeles, CA 90089, USA³Department of Chemistry, University of Florida, Gainesville, FL 32611-7200, USA⁴Present address: Genentech, Inc. 1 DNA Way, South San Francisco, CA 94080, USA⁵Lead Contact*Correspondence: matthew.eddy@ufl.edu<https://doi.org/10.1016/j.str.2020.11.005>

SUMMARY

In drug design, G protein-coupled receptor (GPCR) partial agonists enable one to fine-tune receptor output between basal and maximal signaling levels. Here, we add to the structural basis for rationalizing and monitoring partial agonism. NMR spectroscopy of partial agonist complexes of the A_{2A} adenosine receptor (A_{2A}AR) revealed conformations of the P-I-F activation motif that are distinctly different from full agonist complexes. At the intracellular surface, different conformations of helix VI observed for partial and full agonist complexes manifest a correlation between the efficacy-related structural rearrangement of this activation motif and intracellular signaling to partner proteins. While comparisons of A_{2A}AR in complexes with partial and full agonists with different methods showed close similarity of the global folds, this NMR study now reveals subtle but distinct local structural differences related to partial agonism.

INTRODUCTION

G protein-coupled receptors (GPCRs) initiate a wide range of pharmacological responses, which are largely determined by the efficacies of bound drugs. Drugs known as partial agonists are particularly intriguing as they can activate GPCRs to a sub-maximal level, resulting in a range of receptor activities spanning from basal level signaling to full activation. Development of partial agonist drugs is therefore of interest whenever overstimulation of a GPCR needs to be prevented by tuning the receptor response (Hauser et al., 2017). GPCR partial agonists currently used in the clinic or investigated for their therapeutic potential include drugs targeting opioid receptors (Browne et al., 2020; Chan et al., 2017; Fujimura et al., 2017; Khroyan et al., 2017; Schmid et al., 2017), adrenergic receptors (Calverley et al., 2007), dopamine receptors (Frank et al., 2017; Tarland et al., 2018), and serotonin receptors (Chen et al., 2018; Huang et al., 2017; Yoshinaga et al., 2018; Zheng et al., 2017). Partial agonists are also under consideration as potential treatments for obesity (Wargent et al., 2013) and heart failure (Greene et al., 2016).

The structural basis for partial agonism of GPCRs currently includes five crystal structures of GPCR complexes with partial agonists, which compares with more than 60 crystal and cryoelectron microscopy (cryoEM) structures of different GPCRs, and over 200 structures of complexes of these GPCRs with different

ligands (Pándy-Szekeres et al., 2017). For the few GPCRs where crystal structures are available for complexes with both partial and full agonists, no clear-cut structural differences were observed that would lead to a rationale for distinguishing between partial and full agonism (Warne et al., 2010). In this study, we apply NMR spectroscopy in solution to provide additional insight into the structural basis of partial agonism.

The human A_{2A} adenosine receptor (A_{2A}AR) in complexes with two partial agonists, LUF5834 (Beukers et al., 2004; Lane et al., 2012) and the drug regadenoson, approved by the US Food and Drug Administration (FDA) to evaluate heart conditions (Al Jaroudi and Iskandrian, 2009; Cerqueira, 2004; Noel et al., 2017), was studied with NMR spectroscopy. NMR in solution complements crystal and cryoEM structures of GPCRs by detecting function-related structural plasticity, which may include observing multiple, simultaneously populated conformations that exist in function-related equilibria (Shimada et al., 2019). Previously, evaluation of amide ¹⁵N–¹H signals in well-dispersed 2D [¹⁵N, ¹H]-TROSY (transverse relaxation-optimized spectroscopy) correlation spectra of A_{2A}AR complexes with full agonists and antagonists permitted qualitative comparisons of structural features that correlated with ligand efficacy, whereby detailed mechanistic insight was provided by striking differences observed for the indole ¹⁵N–¹H signals of Trp246^{6.48} (superscripts indicate the Ballesteros-Weinstein nomenclature;



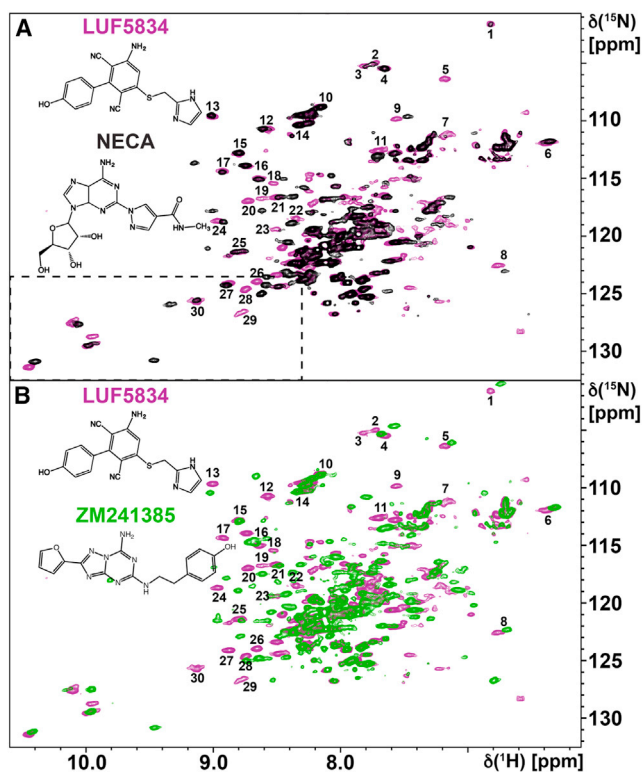


Figure 1. Global Folds of $A_{2A}AR$ Complexes with a Partial Agonist, a Full Agonist, and an Antagonist

(A) 800 MHz ^{15}N , 1H -TROSY correlation spectrum of $[u-^{15}N, \sim 70\% ^2H]$ - $A_{2A}AR$ in complex with the partial agonist LUF5834 (purple) superimposed with that of the complex with the full agonist NECA (black). The region framed with dotted lines corresponds to the region shown on an expanded scale in Figure 2A. On the left the chemical structures of the ligands are shown.

(B) Corresponding superposition for the complexes with LUF5834 (purple) and the antagonist ZM241385 (green).

Ballesteros and Weinstein, 1995), which is located near the highly conserved P-I-F activation motif (Eddy et al., 2018b). For most class A GPCRs, the amino acids Pro^{5.50}, I^{3.40}, and F^{6.44} are clustered together in the receptor structure at the interface between the trans-membrane helices (TMs) V, III, and VI. The relative side chain orientations of these three amino acids are closely related to both the efficacy of bound drugs and to structural rearrangements at the receptor intracellular surface observed in tertiary signaling complexes (Rasmussen et al., 2011; Wacker et al., 2013). Here, 2D ^{15}N , 1H -TROSY correlation spectra revealed novel structural features of the P-I-F activation motif that are linked to the functional efficacy of bound partial agonist drugs.

RESULTS

$A_{2A}AR$ Complexes with Full and Partial Agonists in Solution Share Similar Global Folds

2D ^{15}N , 1H -TROSY correlation spectra of $[u-^{15}N, \sim 70\% ^2H]$ $A_{2A}AR$ complexes with the partial agonists LUF5834 and regadenoson are well resolved and dispersed, allowing detailed comparison with previously reported $A_{2A}AR$ complexes with full agonists and antagonists. The $A_{2A}AR$ complexes with the partial agonist

LUF5834 and the full agonist NECA (5'-(N-Ethylcarboxamido) adenosine) show a high degree of similarity in the distribution of NMR signals, specifically for the well-dispersed signals numbered 1 to 30 (Figure 1A), which have large conformation-dependent contributions to the chemical shifts (Wüthrich, 1986). In the spectral region containing NMR signals with 1H chemical shifts greater than 8.5 ppm, which typically arise from backbone amide ^{15}N - 1H signals in regular secondary structures, the two spectra share a set of signals with similar or identical chemical shifts. The ^{15}N , 1H -TROSY spectrum of $A_{2A}AR$ in complex with regadenoson also shares a closely similar pattern of signals to the spectrum of the complex with NECA (Figure S1). In contrast, between the ^{15}N , 1H -TROSY spectra of $A_{2A}AR$ complexes with the partial agonist LUF5834 and the antagonist ZM241385 these signals are distinctly different (Figure 1B). As the ^{15}N , 1H -TROSY spectra, and specifically the signals 1 to 30 provide a fingerprint of the overall protein conformation, the spectral comparisons in Figure 1 show that the global fold of the $A_{2A}AR$ complex with LUF5834 is more closely related to the global fold of the $A_{2A}AR$ -NECA complex than to the $A_{2A}AR$ -ZM241385 complex.

Indole ^{15}N - 1H NMR Signal of the Toggle Switch Trp246^{6.48} Reports Localized Structural Differences between $A_{2A}AR$ Complexes with Full and Partial Agonists

In earlier NMR studies of $[u-^{15}N, \sim 70\% ^2H]$ $A_{2A}AR$, the chemical shift of the Trp246^{6.48} indole ^{15}N - 1H was observed to strongly correlate with the efficacy of bound drugs (Eddy et al., 2018b). This result was rationalized by ring current effects on the chemical shift (Liu and Wüthrich, 2016; Perkins and Wüthrich, 1979; Wüthrich, 1986) due to Phe242^{6.44} being located near to Trp246^{6.48}. It was thus established that the Trp246^{6.48} indole ^{15}N - 1H NMR signal probes the relative orientation of Phe242^{6.44}, which is part of the highly conserved Pro^{5.50}-Ile^{3.40}-Phe^{6.44} activation motif (Wacker et al., 2013). In the present work, we monitored the Trp246^{6.48} indole ^{15}N and 1H chemical shifts to assess the response of Phe242^{6.44} to the efficacy of bound partial agonists. A single Trp246^{6.48} indole ^{15}N - 1H signal was observed in the ^{15}N , 1H -TROSY spectrum of the $A_{2A}AR$ complex with the partial agonist LUF5834 (Figure 2A). This signal was assigned to Trp246^{6.48} by comparing the spectra of $A_{2A}AR$ and an $A_{2A}AR$ variant containing a W246F point mutation (Figures 2A and 2B) and showing that $A_{2A}AR$ [W246F] retained the global fold of $A_{2A}AR$ (Figure S2). The Trp246^{6.48} indole ^{15}N - 1H signal was now found to be downfield shifted by 2.9 ppm and 0.6 ppm in the ^{15}N and 1H dimensions, respectively, for the LUF5834 complex compared with the NECA complex, and by 4.2 ppm and 1.5 ppm compared with the complex with ZM241385 (Figure 2C). Given the strong dependence of the Trp246^{6.48} indole ^{15}N - 1H chemical shift on the Phe242^{6.44} ring current effects (Liu and Wüthrich, 2016), this suggests that Phe242^{6.44} adopts a unique orientation in the complex with LUF5834 (see below).

The $A_{2A}AR$ Trp246^{6.48} ^{15}N - 1H Indole NMR Chemical Shifts Correlate with the Efficacies of Bound Partial and Full Agonists

Regadenoson, known also as CVT-3146, has been documented as having an efficacy more similar to a full agonist than the partial

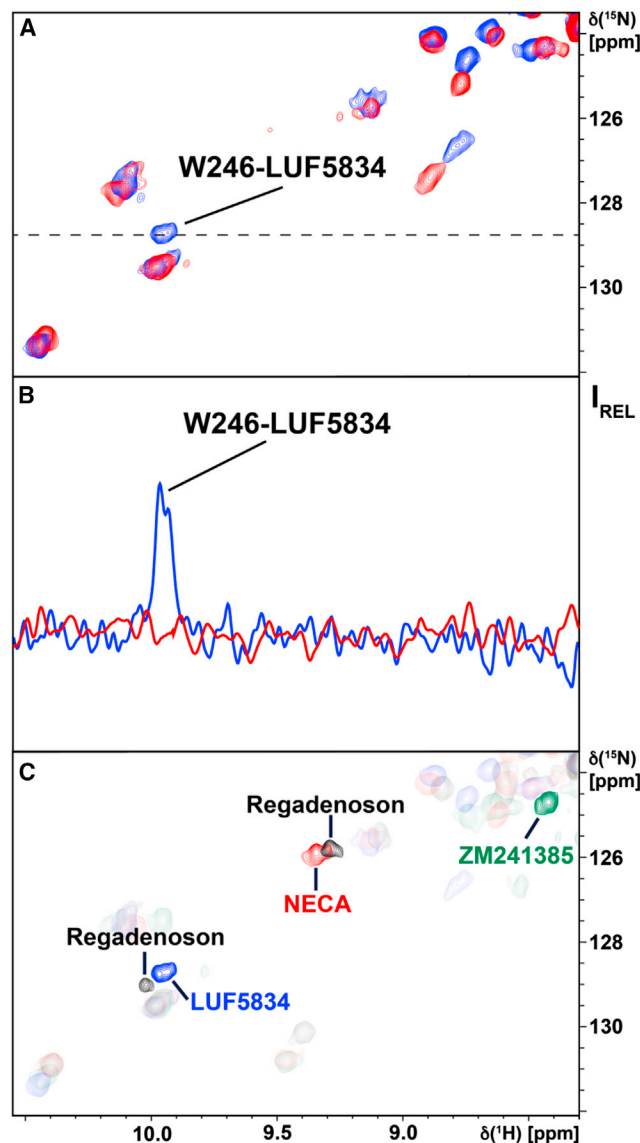


Figure 2. Manifestation of $A_{2A}\text{AR}$ Partial Agonism in the Toggle Switch Tryptophan Indole ^{15}N - ^1H NMR Signal

(A and B) Assignment of the Trp246^{6,48} indole ^{15}N - ^1H NMR signal of $A_{2A}\text{AR}$ in complex with the partial agonist LUF5834 by its absence in the spectrum of $A_{2A}\text{AR}$ [W246F]. (A) Superposition of the indole ^{15}N - ^1H region in contour plots of 800 MHz 2D [^{15}N , ^1H]-TROSY correlation spectra of [u - ^{15}N , $\sim 70\%$ ^2H]- $A_{2A}\text{AR}$ (blue) and [u - ^{15}N , $\sim 70\%$ ^2H]- $A_{2A}\text{AR}$ [W246F] (red). (B) 1D cross sections at the ^{15}N chemical shift indicated by the horizontal dashed line in (A).

(C) The indole ^{15}N - ^1H regions of four 800 MHz 2D [^{15}N , ^1H]-TROSY correlation spectra are superimposed, highlighting the Trp246^{6,48} indole ^{15}N - ^1H NMR signal of the $A_{2A}\text{AR}$ complexes with the antagonist ZM241385 (green), the partial agonist regadenoson (black), the partial agonist LUF5834 (blue), and the full agonist NECA (red). For improved clarity, the opacity of all other signals in the displayed spectral region has been reduced.

agonist LUF5834 (Gao et al., 2001). In 2D [^{15}N , ^1H]-TROSY spectra of the $A_{2A}\text{AR}$ complex with regadenoson, two lines of different intensities were observed for the Trp246^{6,48} indole ^{15}N - ^1H signal. The line of lesser intensity has chemical shifts similar to the indole ^{15}N - ^1H signal of the $A_{2A}\text{AR}$ complex with

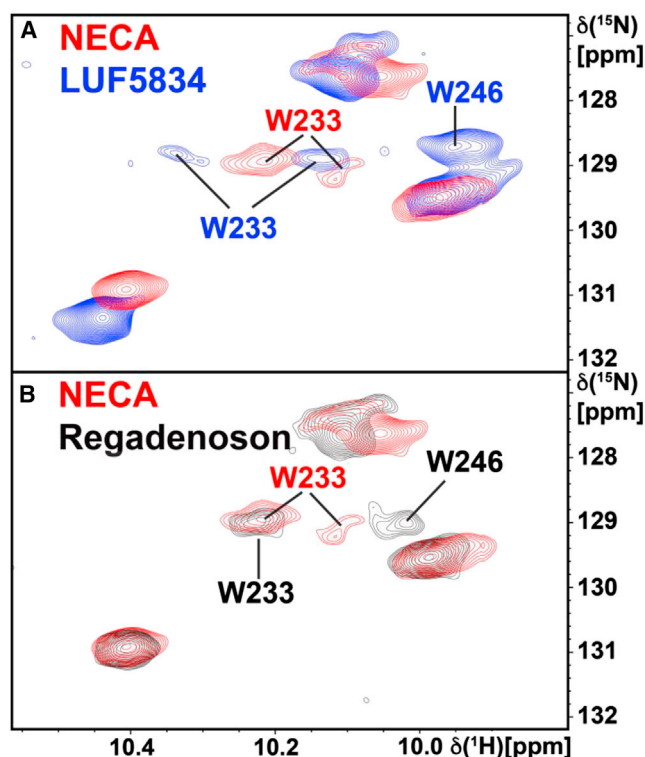


Figure 3. Engineered NMR Probe Trp233 at the Intracellular Surface of $A_{2A}\text{AR}$ Manifests Variable Efficacies of Full and Partial Agonists

(A) Superposition of contour plots of the Trp indole ^{15}N - ^1H region in 800 MHz 2D [^{15}N , ^1H]-TROSY correlation spectra of [u - ^{15}N , $\sim 70\%$ ^2H]- $A_{2A}\text{AR}$ [K233W] in complexes with NECA (red) and LUF5834 (blue).

(B) Corresponding superposition as in (A) for the $A_{2A}\text{AR}$ complexes with NECA (red) and regadenoson (black).

LUF5834, and the line of greater intensity has chemical shifts similar to the indole ^{15}N - ^1H signal for complexes with full agonists (Figure 2C). This represents two simultaneously populated protein conformations, where one is similar to that observed for full agonists and the other one has a similar conformation to that observed for the complex with the partial agonist LUF5834. The higher population of the NECA-like conformation is in line with the near-full agonist efficacy of regadenoson.

Intracellular $A_{2A}\text{AR}$ Surface Response to Bound Partial Agonists

To probe the response of the $A_{2A}\text{AR}$ intracellular signaling surface to bound partial agonists, we measured 2D [^{15}N , ^1H]-TROSY correlation spectra of an $A_{2A}\text{AR}$ variant containing an engineered tryptophan at position 233 in helix VI near the intracellular surface, $A_{2A}\text{AR}$ [K233W]. The indole ^{15}N - ^1H NMR signal of this extrinsic tryptophan was previously demonstrated to be well resolved and sensitive to the efficacy of drugs bound to $A_{2A}\text{AR}$ (Eddy et al., 2018a).

In 2D [^{15}N , ^1H]-TROSY correlation spectra of [u - ^{15}N , $\sim 70\%$ ^2H]- $A_{2A}\text{AR}$ [K233W] in complex with the partial agonist LUF5834, two signals with different intensities were observed at ^1H chemical shifts of ~ 10.1 and ~ 10.3 ppm (Figure 3A). The signal at 10.1 ppm has a similar chemical shift as one of

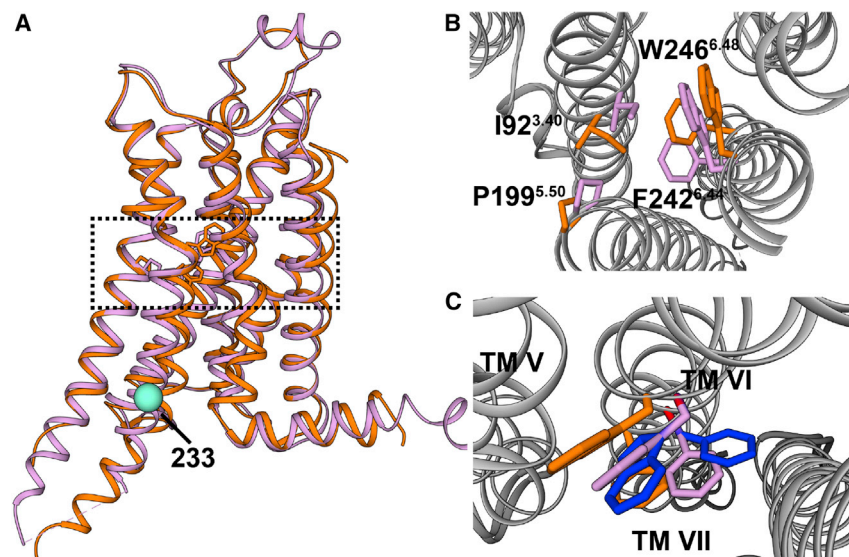


Figure 4. Location of the P-I-F Activation Microswitch in $A_{2A}AR$ and Spatial Arrangement of the Toggle Switch Trp246^{6.48} and Phe242^{6.44} that are Compatible with Ring Current Shift Calculations Using the Atomic Coordinates of an $A_{2A}AR$ Partial Agonist Complex Model.

(A) Crystal structures of $A_{2A}AR$ in complexes with the full agonist NECA (purple; PDB: 2YDV) and the antagonist ZM241385 (orange; PDB: 3EML) are superimposed. The dotted black box shows the location of the P-I-F activation microswitch in the protein structures and the cyan-colored sphere identifies the amino acid position 233.

(B) Top-down expanded view of the P-I-F activation microswitch and the nearby Trp246^{6.48}. The protein backbone is colored gray, and the annotated side chains for the complexes with NECA and ZM241385 are purple and orange, respectively. The protein backbone segments located above the annotated amino acids were removed for improved clarity.

(C) A ring current shift-derived model of the complex with the partial agonist LUF5834 (blue) superimposed on the $A_{2A}AR$ structures presented in (B). In the LUF5834 complex, the Trp246^{6.48} χ^2 angle is rotated by -20° and the F242^{6.44} χ^1 angle by $+60^\circ$ relative to the orientations in the NECA complex (Table S1).

two signal components observed for the analogous complex with the full agonist NECA (Figure 3A). In a 2D [¹⁵N, ¹H]-TROSY correlation spectrum of [^u-¹⁵N, ~70% ²H]- $A_{2A}AR$ [K233W] in complex with the partial agonist regadenoson, only one signal was observed at a ¹H chemical shift of 10.2 ppm, which is similar to the chemical shift of the signal arising from the more highly populated state of the complex with NECA (Figure 3B).

Figure 3 leads to a rather unexpected observation. It shows one dominantly populated conformation for the $A_{2A}AR$ complexes with each of the three ligands NECA, LUF5834, and regadenoson. In addition, a lesser populated conformation is seen for the NECA and LUF5834 complexes, whereas no minor conformation is seen when regadenoson is bound. We conclude that the dominant conformation is indicative of the major signaling pathway induced by the ligand. The full agonist NECA and the partial agonist regadenoson thus appear to have identical dominant signaling pathways, whereas the major signaling pathway of LUF5834 coincides with the minor component of NECA. Overall, we arrive at the observation that NECA has a minor signaling component that coincides with the major pathway of LUF5834, whereas the signaling by regadenoson appears to be a pure pathway characteristic of a full agonist.

Structural Models of Trp246^{6.48} Interactions with Phe242^{6.44} in $A_{2A}AR$ Partial Agonist Complexes Derived from NMR Ring Current Effects

Ring current effects (Wüthrich, 1986) contributing to the Trp246^{6.48} indole ¹⁵N-¹H chemical shifts were calculated with the program MOLMOL (Koradi et al., 1996), using the atomic coordinates of crystal structures of $A_{2A}AR$ complexes with different ligands (Doré et al., 2011; Jaakola et al., 2008; Lebon et al., 2011, 2015; Xu et al., 2011) (Table S1). The ring current shifts calculated for the entire protein (Table S1) showed that Phe242^{6.44} is the major contributor to the observed effect.

For the structures of the $A_{2A}AR$ complexes included in Table S1, the calculated chemical shifts for the Trp246^{6.48} indole ¹⁵N-¹H signal were all significantly upfield from the experimentally observed chemical shifts for the complex with LUF5834. Hence, the relative orientations of Phe242^{6.44} and Trp246^{6.48} in this partial agonist complex must be different from those in $A_{2A}AR$ complexes with either antagonists or agonists. To obtain a structural interpretation of this observation, a series of molecular models were generated by independently varying χ^1 of Trp246^{6.48} in 10° increments, and χ^1 and χ^2 of Phe242^{6.44} by 10° increments each, and calculating the ring current shifts for the resulting relative orientations of the two amino acids. For most of the thus generated relative orientations of Trp246^{6.48} and Phe242^{6.44}, steric clashes with overlap of the van der Waals radii by more than 0.6 Å were observed between the Trp246^{6.48} side chain and the spatially proximate residues Thr88^{3.36} in helix III and Ser277^{7.42} in helix VII. These orientations of Trp246^{6.48} would require substantial reorientation of these spatially proximate residues. Among the generated local structures that did not show steric clashes, only a narrow range of Trp246^{6.48} and Phe242^{6.44} side chain orientations yielded ring current shifts that represent a close fit with the observed chemical shifts. As an illustration, Figure 4 shows the structural model where Trp246^{6.48} χ^2 is rotated by -20° and F242^{6.44} χ^1 by $+60^\circ$ relative to the orientations in the NECA complex (see also Table S1).

DISCUSSION

The NMR data of Figures 1, 2, and 3 reveal a clear-cut correlation between the structural response to bound full and partial agonists by the P-I-F activation switch in $A_{2A}AR$, as observed with Trp246^{6.48} serving as a naturally built-in NMR probe, and the tip of TM VI at the intracellular surface, as recorded with the engineered Trp233 probe. This correlation provides a new window

into mechanisms of GPCR activation by partial agonists and indicates that differences in efficacy between full and partial agonists are linked to different pathways of propagating information from the orthosteric drug binding pocket to signaling-related conformational changes at the intracellular surface. For the complex with regadenoson, two signals were observed for Trp246^{6,48}, indicating the presence of two locally different A_{2A}AR conformations, where the dominantly populated conformation of the P-I-F activation switch more closely resembles that of the complex with the full agonist NECA, and a lesser populated state more closely resembles that of the partial agonist LUF5834. For Trp233 at the intracellular surface, only one signal is observed for the complex with regadenoson. It would thus appear that, in passing from the activation switch to the intracellular surface, one of the two potential signaling pathways is attenuated, leading to a slightly reduced drug efficacy compared with NECA but otherwise exhibiting the behavior of a full agonist. On the other hand, at the intracellular surface of TM VI, the complex with NECA shows a small admixture of a state that corresponds to the dominant conformation observed for the complex with LUF5834. This indicates that the conformational ensemble of the A_{2A}AR complex with this full agonist includes a small population of the state that is characteristic of the structure at the signaling surface of the complex with a typical partial agonist.

The indications of a unique orientation of Phe242^{6,44} and a unique local structure at the intracellular tip of helix VI indicate that, in the absence of interactions with intracellular partner proteins, A_{2A}AR complexes with partial agonists already adopt a conformation that differs in subtle but critical ways from the conformation of the agonist complexes. Conformational rearrangement of Phe^{6,44} between complexes with antagonists and agonists is correlated with rearrangement of the conformations of Ile^{3,40} and Pro^{5,50} to avoid steric hindrances among these bulkier amino acids, which has been postulated to trigger the rotation of helix VI near the intracellular surface (Wacker et al., 2013). Extending these observations to the present study implies that Ile^{3,40} and Pro^{5,50} in complexes with partial agonists are also present in orientations that are distinct from agonist and antagonist complexes; this could lead to a unique orientation of helix VI for partial agonist complexes. An interplay between Phe^{6,44} and Trp246^{6,48} may also contribute to the mechanism of partial agonism through interactions with Asp^{2,50}. Earlier NMR studies demonstrated the existence of a function-related interplay between Asp52^{2,50} and Trp246^{6,48} (Eddy et al., 2018b). Replacement of Asp^{2,50} with Asn at the same position resulted in a loss of G protein signaling and a perturbation of the local environment around Trp246^{6,48} (Eddy et al., 2018b). Interactions between Asp^{2,50} and Trp^{6,48} were subsequently observed in crystal structures of the human endothelin receptor ETB bound to full and partial agonists (Shihoya et al., 2018). Differences in interactions between Asp^{2,50} and Trp^{6,48} in complexes with full and partial agonists were postulated to be related to changes in other known activation motifs such as the NPxxY motif in helix VII (Shihoya et al., 2018).

The present NMR results are in line with data on GPCR complexes with partial agonists that were previously obtained with different experimental methods, and provide key [Supplemental Information](#). In a crystallographic study of the β_1 -adrenergic receptor (β_1 AR), comparison between complexes with full and par-

tial agonists revealed a difference of one hydrogen bond between the bound ligands and interacting amino acids in the orthosteric ligand binding pocket, while the P-I-F activation motif and the intracellular surface were nearly identical in complexes with full and partial agonists (Warne et al., 2010). These studies may have been affected by the use of multiple stabilizing mutations to facilitate crystallization, whereas A_{2A}AR and A_{2A}AR variants used in the present study did not contain any thermostabilizing mutations. For the β_2 -adrenergic receptor (β_2 AR), the structure of a ternary complex with the partial agonist salmeterol and a G protein-mimicking nanobody was found to be closely similar to a ternary complex with a full agonist and a G protein, whereas there were larger differences compared with an antagonist complex (Masureel et al., 2018). Specifically, TM VI was to a lesser extent displaced outward, relative to the antagonist complex, in the complex with the partial agonist than in the ternary complex with full agonist and a G protein (Masureel et al., 2018). The conformation of the P-I-F activation motif was observed to be nearly identical between β_2 AR complexes with full and partial agonists.

Evidence from fluorescence spectroscopic studies and GDP binding experiments support the idea that, depending on whether a partial or full agonist is bound, receptors form different conformations with partner G proteins. Thus, nucleotide exchange measurements for ternary GPCR complexes demonstrated that G proteins have high affinities for GDP when their partner GPCR is bound to a partial agonist, thereby decreasing the rate of nucleotide exchange required for intracellular signaling (Roberts et al., 2004; Seifert et al., 1999; Zhang et al., 2004). Single molecule fluorescence spectroscopic studies of β_2 AR provided evidence for different helix VI conformations at the intracellular surface for complexes with partial or full agonist (Gregorio et al., 2017), which is consistent with earlier studies reporting different fluorescence responses for β_2 AR bound to full or partial agonists (Gether et al., 1995). Overall, while being compatible with previously published structural data on partial agonists, the NMR data presented in this paper now provide detailed insights into mechanistic aspects of partial agonist signaling.

STAR★METHODS

Detailed methods are provided in the online version of this paper and include the following:

- KEY RESOURCES TABLE
- RESOURCE AVAILABILITY
 - Lead Contact
 - Materials Availability
 - Data and Code Availability
- EXPERIMENTAL MODEL AND SUBJECT DETAILS
 - Microbes
 - Cell Lines
- METHOD DETAILS
 - Mutagenesis
 - Protein Production
 - NMR Sample Preparation
 - NMR Spectroscopy
- QUANTIFICATION AND STATISTICAL ANALYSIS
- ADDITIONAL RESOURCES

SUPPLEMENTAL INFORMATION

Supplemental Information can be found online at <https://doi.org/10.1016/j.str.2020.11.005>.

ACKNOWLEDGMENTS

The authors acknowledge support from the NIH/NIGMS (R01GM115825). M.T.E. acknowledges former financial support from Dr. Raymond Stevens (USC) and from an ACS postdoctoral fellowship (award ID: 126774-PF-14-178-01-DMC) and current support from the NIH/NIGMS Maximizing Investigators' Research Award (MIRA) R35, 1R35GM138291. K.W. is the Cecil and Ida M. Green Professor of Structural Biology at The Scripps Research Institute.

AUTHOR CONTRIBUTIONS

M.T.E. and K.W. designed the project. M.T.E. and B.M. performed protein purification, sample characterization, and measurements of NMR data. M.T.E., B.M., and K.W. analyzed NMR data. M.T.E. and K.W. wrote the manuscript with input from B.M.

DECLARATION OF INTERESTS

The authors declare no competing interests.

Received: July 7, 2020

Revised: September 13, 2020

Accepted: November 3, 2020

Published: November 24, 2021

REFERENCES

- Al Jaroudi, W., and Iskandrian, A.E. (2009). Regadenoson: a new myocardial stress agent. *J. Am. Coll. Cardiol.* *54*, 1123–1130.
- Ballesteros, J., and Weinstein, H. (1995). Integrated methods for modeling G-protein coupled receptors. *Methods Neurosci.* *25*, 366–428.
- Beukers, M.W., Chang, L.C.W., von Frijtag Drabbe Künzel, J.K., Mulder-Krieger, T., Spanjersberg, R.F., Brussee, J., and IJzerman, A.P. (2004). New, non-adenosine, high-potency agonists for the human adenosine A2B receptor with an improved selectivity profile compared to the reference agonist n-ethylcarboxamidoadenosine. *J. Med. Chem.* *47*, 3707–3709.
- Browne, C.A., Smith, T., and Lucki, I. (2020). Behavioral effects of the kappa opioid receptor partial agonist nalmefene in tests relevant to depression. *Eur. J. Pharmacol.* *872*, 1–7.
- Calverley, P.M.A., Anderson, J.A., Celli, B., Ferguson, G.T., Jenkins, C., Jones, P.W., Yates, J.C., and Vestbo, J. (2007). Salmeterol and fluticasone propionate and survival in chronic obstructive pulmonary disease. *N. Engl. J. Med.* *356*, 775–789.
- Cerqueira, M.D. (2004). The future of pharmacologic stress: selective A2A adenosine receptor agonists. *Am. J. Cardiol.* *94*, 33–40.
- Chan, H.C.S., McCarthy, D., Li, J., Palczewski, K., and Yuan, S. (2017). Designing safer analgesics via μ -opioid receptor pathways. *Trends Pharmacol. Sci.* *38*, 1016–1037.
- Chen, X.-f., Jin, Z.-l., Gong, Y., Zhao, N., Wang, X.-y., Ran, Y.-h., Zhang, Y.-z., Zhang, L.-m., and Li, Y.-f. (2018). 5-HT6 receptor agonist and memory-enhancing properties of hypidone hydrochloride (yl-0919), a novel 5-HT1A receptor partial agonist and SSRI. *Neuropharmacology* *138*, 1–9.
- Doré, A.S., Robertson, N., Errey, J.C., Ng, I., Hollenstein, K., Tehan, B., Hurrell, E., Bennett, K., Congreve, M., Magnani, F., et al. (2011). Structure of the adenosine A2A receptor in complex with zm241385 and the xanthines xac and caffeine. *Structure* *19*, 1283–1293.
- Eddy, M.T., Gao, Z.-G., Mannes, P., Patel, N., Jacobson, K.A., Katritch, V., Stevens, R.C., and Wüthrich, K. (2018a). Extrinsic tryptophans as NMR probes of allosteric coupling in membrane proteins: application to the A2A adenosine receptor. *J. Am. Chem. Soc.* *140*, 8228–8235.
- Eddy, M.T., Lee, M.Y., Gao, Z.G., White, K.L., Didenko, T., Horst, R., Audet, M., Stanczak, P., McClary, K.M., Han, G.W., et al. (2018b). Allosteric coupling of drug binding and intracellular signaling in the A_{2A} adenosine receptor. *Cell* *172*, 68–80.
- Frank, G.K.W., Shott, M.E., Hagman, J.O., Schiel, M.A., DeGuzman, M.C., and Rossi, B. (2017). The partial dopamine D2 receptor agonist aripiprazole is associated with weight gain in adolescent anorexia nervosa. *Int. J. Eat. Disord.* *50*, 447–450.
- Fujimura, M., Izumimoto, N., Kanie, S., Kobayashi, R., Yoshikawa, S., Momen, S., Hirakata, M., Komagata, T., Okanishi, S., Iwata, M., et al. (2017). Mechanisms of inhibitory action of TRK-130 (naltalimide), a μ -opioid receptor partial agonist, on the micturition reflex. *Int. Urol. Nephrol.* *49*, 587–595.
- Gao, Z., Li, Z., Baker, S.P., Lasley, R.D., Meyer, S., Elzein, E., Palle, V., Zablocki, J.A., Blackburn, B., and Belardinelli, L. (2001). Novel short-acting A2A adenosine receptor agonists for coronary vasodilation: inverse relationship between affinity and duration of action of A2A agonists. *J. Pharmacol. Exp. Ther.* *298*, 209–218.
- Gether, U., Lin, S., and Kobilka, B.K. (1995). Fluorescent labeling of purified beta 2 adrenergic receptor. Evidence for ligand-specific conformational changes. *J. Biol. Chem.* *270*, 28268–28275.
- Greene, S.J., Sabbah, H.N., Butler, J., Voors, A.A., Albrecht-Küpper, B.E., Dünge, H.D., Dinh, W., and Gheorghade, M. (2016). Partial adenosine A1 receptor agonism: a potential new therapeutic strategy for heart failure. *Heart Fail Rev.* *21*, 95–102.
- Gregorio, G.G., Masureel, M., Hilger, D., Terry, D.S., Juette, M., Zhao, H., Zhou, Z., Perez-Aguilar, J.M., Hauge, M., Mathiasen, S., et al. (2017). Single-molecule analysis of ligand efficacy in β_2 AR-G-protein activation. *Nature* *547*, 68–73.
- Hauser, A.S., Attwood, M.M., Rask-Andersen, M., Schiöth, H.B., and Gloriam, D.E. (2017). Trends in GPCR drug discovery: new agents, targets and indications. *Nat. Rev. Drug Discov.* *16*, 829–842.
- Huang, X., Yang, J., Yang, S., Cao, S., Qin, D., Zhou, Y., Li, X., Ye, Y., and Wu, J. (2017). Role of tandospirone, a 5-HT1A receptor partial agonist, in the treatment of central nervous system disorders and the underlying mechanisms. *Oncotarget* *8*, 102705–102720.
- Jaakola, V.-P., Griffith, M.T., Hanson, M.A., Cherezov, V., Chien, E.Y.T., Lane, J.R., IJzerman, A.P., and Stevens, R.C. (2008). The 2.6 angstrom crystal structure of a human A2A adenosine receptor bound to an antagonist. *Science* *322*, 1211–1217.
- Khroyan, T.V., Cippitelli, A., Toll, N., Lawson, J.A., Crossman, W., Polgar, W.E., and Toll, L. (2017). In vitro and in vivo profile of PPL-101 and PPL-103: mixed opioid partial agonist analgesics with low abuse potential. *Front. Psychiatry* *8*, 7215–7285.
- Koradi, R., Billeter, M., and Wüthrich, K. (1996). Molmol: a program for display and analysis of macromolecular structures. *J. Mol. Graphics* *14*, 51–55.
- Lane, J.R., Klein Herenbrink, C., van Westen, G.J.P., Spoorenndonk, J.A., Hoffmann, C., and IJzerman, A.P. (2012). A novel nonribose agonist, LUF5834, engages residues that are distinct from those of adenosine-like ligands to activate the adenosine A2A receptor. *Mol. Pharmacol.* *81*, 475–487.
- Lebon, G., Edwards, P.C., Leslie, A.G.W., and Tate, C.G. (2015). Molecular determinants of cgs21680 binding to the human adenosine A2A receptor. *Mol. Pharmacol.* *87*, 907–915.
- Lebon, G., Warne, T., Edwards, P.C., Bennett, K., Langmead, C.J., Leslie, A.G.W., and Tate, C.G. (2011). Agonist-bound adenosine A2A receptor structures reveal common features of GPCR activation. *Nature* *474*, 521–525.
- Liu, D., and Wüthrich, K. (2016). Ring current shifts in 19F-NMR of membrane proteins. *J. Biomol. NMR* *65*, 1–5.
- Masureel, M., Zou, Y., Picard, L.-P., van der Westhuizen, E., Mahoney, J.P., Rodrigues, J.P.G.L.M., Mildorf, T.J., Dror, R.O., Shaw, D.E., Bouvier, M., et al. (2018). Structural insights into binding specificity, efficacy and bias of a β_2 AR partial agonist. *Nat. Chem. Biol.* *14*, 1059–1066.
- Noel, C.V., Krishnamurthy, R., Moffett, B., and Krishnamurthy, R. (2017). Myocardial stress perfusion magnetic resonance: initial experience in a

- pediatric and young adult population using regadenoson. *Pediatr. Radiol.* **47**, 280–289.
- Pándy-Szekeres, G., Munk, C., Tsonkov, T.M., Mordalski, S., Harpsøe, K., Hauser, A.S., Bojarski, A.J., and Gloriam, D.E. (2017). GPCRdb in 2018: adding GPCR structure models and ligands. *Nucleic Acids Res.* **46**, D440–D446.
- Perkins, S.J., and Wüthrich, K. (1979). Ring current effects in the conformation dependent NMR chemical shifts of aliphatic protons in the basic pancreatic trypsin inhibitor. *Biochim. Biophys. Acta* **576**, 409–423.
- Pervushin, K., Riek, R., Wider, G., and Wüthrich, K. (1997). Attenuated t2 relaxation by mutual cancellation of dipole-dipole coupling and chemical shift anisotropy indicates an avenue to NMR structures of very large biological macromolecules in solution. *Proc. Natl. Acad. Sci.* **94**, 12366–12371.
- Rasmussen, S.G.F., DeVree, B.T., Zou, Y., Kruse, A.C., Chung, K.Y., Kobilka, T.S., Thian, F.S., Chae, P.S., Pardon, E., Calinski, D., et al. (2011). Crystal structure of the β_2 adrenergic receptor-gs protein complex. *Nature* **477**, 549–555.
- Roberts, D.J., Lin, H., and Strange, P.G. (2004). Mechanisms of agonist action at D2 dopamine receptors. *Mol. Pharmacol.* **66**, 1573–1579.
- Schmid, C.L., Kennedy, N.M., Ross, N.C., Lovell, K.M., Yue, Z., Morgenweck, J., Cameron, M.D., Bannister, T.D., and Bohn, L.M. (2017). Bias factor and therapeutic window correlate to predict safer opioid analgesics. *Cell* **171**, 1165–1175.
- Seifert, R., Gether, U., Wenzel-Seifert, K., and Kobilka, B.K. (1999). Effects of guanine, inosine, and xanthine nucleotides on β_2 -adrenergic receptor/gs interactions: evidence for multiple receptor conformations. *Mol. Pharmacol.* **56**, 348–358.
- Shihoya, W., Izume, T., Inoue, A., Yamashita, K., Kadji, F.M.N., Hirata, K., Aoki, J., Nishizawa, T., and Nureki, O. (2018). Crystal structures of human ETB receptor provide mechanistic insight into receptor activation and partial activation. *Nat. Commun.* **9**, 1–11.
- Shimada, I., Ueda, T., Kofuku, Y., Eddy, M.T., and Wüthrich, K. (2019). GPCR drug discovery: Integrating solution NMR data with crystal and cryo-EM structures. *Nat. Rev. Drug Discov.* **18**, 59–82.
- Tarland, E., Franke, R.T., Fink, H., Pertz, H.H., and Brosda, J. (2018). Effects of 2-bromoterguride, a dopamine D2 receptor partial agonist, on cognitive dysfunction and social aversion in rats. *Psychopharmacology* **235**, 99–108.
- Wacker, D., Wang, C., Katritch, V., Han, G.W., Huang, X.P., Vardy, E., McCorvy, J.D., Jiang, Y., Chu, M., Siu, F.Y., et al. (2013). Structural features for functional selectivity at serotonin receptors. *Science* **340**, 615–619.
- Wargent, E.T., Zaibi, M.S., Silvestri, C., Hislop, D.C., Stocker, C.J., Stott, C.G., Guy, G.W., Duncan, M., Di Marzo, V., and Cawthorne, M.A. (2013). The cannabinoid $\delta(9)$ -tetrahydrocannabivarin (THCV) ameliorates insulin sensitivity in two mouse models of obesity. *Nutr. Diabetes* **3**, e68–e78.
- Warne, T., Moukhametzianov, R., Baker, J.G., Nehmé, R., Edwards, P.C., Leslie, A.G.W., Schertler, G.F.X., and Tate, C.G. (2010). The structural basis for agonist and partial agonist action on a β_1 -adrenergic receptor. *Nature* **469**, 241–244.
- Wüthrich, K. (1986). *NMR of Proteins and Nucleic Acids* (John Wiley & Sons).
- Xu, F., Wu, H., Katritch, V., Han, G.W., Jacobson, K.A., Gao, Z.-G., Cherezov, V., and Stevens, R.C. (2011). Structure of an agonist-bound human A2A adenosine receptor. *Science* **332**, 322–327.
- Yoshinaga, H., Nishida, T., Sasaki, I., Kato, T., Oki, H., Yabuuchi, K., and Toyoda, T. (2018). Discovery of dsp-1053, a novel benzylpiperidine derivative with potent serotonin transporter inhibitory activity and partial 5-HT1A receptor agonistic activity. *Bioorg. Med. Chem.* **26**, 1614–1627.
- Zhang, Q., Okamura, M., Guo, Z.-D., Niwa, S., and Haga, T. (2004). Effects of partial agonists and Mg²⁺ ions on the interaction of M2 muscarinic acetylcholine receptor and G protein $\alpha i1$ subunit in the M2- $\alpha i1$ fusion protein. *J. Biochem.* **135**, 589–596.
- Zheng, G., Xue, W., Yang, F., Zhang, Y., Chen, Y., Yao, X., and Zhu, F. (2017). Revealing vilazodone's binding mechanism underlying its partial agonism to the 5-HT1A receptor in the treatment of major depressive disorder. *Phys. Chem. Chem. Phys.* **19**, 28885–28896.

STAR★METHODS

KEY RESOURCES TABLE

REAGENT or RESOURCE	SOURCE	IDENTIFIER
Bacterial and Virus Strains		
XL10-Gold ultracompetent cells	Agilent	Cat#200314
Chemicals, Peptides, and Recombinant Proteins		
Cholesteryl hemisuccinate (CHS)	Sigma-Aldrich	Cat#C6512
Lauryl Maltose Neopentyl Glycol (LMNG)	Anatrace	Cat#NG310
ATP	Sigma-Aldrich	Cat#A2383
YNB (without amino acids and ammonium sulfate)	Sigma-Aldrich	Cat#Y1251
Biotin	Sigma-Aldrich	Cat#B4639
4-(2-[7-Amino-2-(2-furyl)[1,2,4]triazolo[2,3-a][1,3,5]triazin-5-ylamino]ethyl)phenol (ZM241385)	Tocris	Cat#1036
5'-N-Ethylcarboxamidoadenosine (NECA)	Tocris	Cat#1691
2-Amino-4-(4-hydroxyphenyl)-6-[(1 <i>H</i> -imidazol-2-ylmethyl)thio]-3,5-pyridinecarbonitrile (LUF 5834)	Tocris	Cat#1063
4-[2-[[6-Amino-9-(<i>N</i> -ethyl-β-D-ribofuranuronamidoyl)-9 <i>H</i> -purin-2-yl]amino]ethyl]benzenepropanoic acid hydrochloride (CGS21680)	Tocris	Cat#4603
Regadenoson	Apex Bio	Cat#B5904
Theophylline	Sigma-Aldrich	Cat#T1633
Iodoacetamide	Sigma-Aldrich	Cat#I1149
TALON Metal Affinity Resin	Clontech	Cat#635504
Deposited Data		
Thermostabilized A _{2A} AR in complex with NECA	Lebon et al. 2011	PDB:2YDV
A _{2A} AR bound to ZM241385	Jaakola et al. 2008	PDB:3EML
Thermostabilized A _{2A} AR in complex with XAC	Doré et al. 2011	PDB:3REY
A _{2A} AR bound to UK432097	Xu et al. 2011	PDB:3QAK
Thermostabilized A _{2A} AR in complex with CGS21680	Lebon et al. 2015	PDB:4UHR
Thermostabilized A _{2A} AR in complex with caffeine	Doré et al. 2011	PDB:3RFM
Experimental Models: Organisms/Strains		
<i>P. pastoris</i> : Bg12	BioGrammatics	Cat#PS004-01
Oligonucleotides		
A _{2A} AR_W246F_F: CATTGTGGGGCTCTTTGCCCTCTGCTTCCTGCCCTACACATCATCAACTGCT	IDT	n/a
A _{2A} AR_W246F_R: AGCAGTTGATGATGTGTAGGGGCAGGAAGCAGAGGGCAAAGAGCCCCA CAATG	IDT	n/a
Recombinant DNA		
Plasmid: human A _{2A} AR(1-316) in pPIC9K	Eddy et al. 2018a	n/a
Plasmid: human A _{2A} AR[W246F]	This study	n/a
Plasmid: human A _{2A} AR[K233W]	Eddy et al. 2018b	
Software and Algorithms		
Topspin v. 3.6.1	Bruker	https://www.bruker.com/products/mr/nmr/nmr-software
Other		
PD-10 column	GE Healthcare	Cat#17085101
Amicon ultra-15 centrifugal filter unit, 30,000 MWCO	Millipore	UFC903024

RESOURCE AVAILABILITY

Lead Contact

Lead Contact: Dr. Matthew Eddy (matthew.eddy@ufl.edu). Further information and requests for resources or reagents should be directed to and will be fulfilled by the Lead Contact.

Materials Availability

All unique reagents generated in this study are available from the Lead Contact by request and with a completed Materials Transfer Agreement.

Data and Code Availability

All other data are available from the corresponding author upon reasonable request.

EXPERIMENTAL MODEL AND SUBJECT DETAILS

Microbes

XL10-Gold *E. coli* cells were cultured in LB medium, and the Bg12 strain of *P. pastoris* cells were cultured in BMGY and BMMY media.

Cell Lines

All cell lines used in this study were authenticated by the suppliers and were chosen to remain consistent with previous studies.

METHOD DETAILS

Mutagenesis

PCR-based site-directed mutagenesis (QuikChange II, Agilent Technologies, CA) was used to generate A_{2A}AR variants with single amino acid replacements used for NMR assignments. Primers used for this effort are provided in the [Key Resources Table](#).

Protein Production

A_{2A}AR was produced from a gene encoding human A_{2A}AR (1-316) containing a point mutation to remove the only glycosylation site N154Q, an N-terminal FLAG tag, and a 10 X C-terminal His tag was cloned into a pPIC9K vector (Invitrogen) at the BamHI and NotI restriction sites. The pharmacological response of this protein expressed in *Pichia* was previously assessed and determined to be functionally identical to A_{2A}AR produced in insect cells (Eddy et al., 2018b). All A_{2A}AR plasmids used in this study were transformed by electroporation into the BG12 strain of *Pichia pastoris* (Biogrammatix, Carlsbad, CA). Protein expression was screened via identical methods to previously published protocols (Eddy et al., 2018b), which utilized anti-FLAG Western Blots to identify colonies with higher expression levels of A_{2A}AR in small scale cultures.

Production of deuterated, ¹⁵N stable-isotope labeled A_{2A}AR samples followed previously established protocols (Eddy et al., 2018b), whereby *Pichia* cells were adapted to increasing amounts of D₂O in BMGY media at 30°C over a 9-day period. Adapted cells were grown in BMGY media containing 99.8% D₂O and ¹⁵N ammonium sulfate and protein expression was carried out in BMMY media containing 99.8% D₂O and ¹⁵N ammonium sulfate.

NMR Sample Preparation

Preparation of A_{2A}AR samples for NMR studies was performed according to previously reported protocols (Eddy et al., 2018b), whereby first A_{2A}AR-containing cell pellets were resuspended in lysis buffer (50 mM sodium phosphate pH 7.0, 100 mM NaCl, 5% glycerol (w/v), and in-house prepared protease cocktail solutions), broken by two passes through a cell disruptor (Constant Systems) and isolated by ultracentrifugation at 200,000 x g. Isolated membranes were resuspended in buffer (10 mM HEPES pH 7.0, 10 mM KCl, 20 mM MgCl₂) then treated with 1 mM theophylline, protease inhibitor cocktail (prepared in-house), and 2 mg/mL iodoacetamine for 1 hour. Subsequently, protein was then extracted by mixing resuspended membranes 1:1 (v/v) with solubilization buffer containing 1% (w/v) 2,2-didodecylpropane-1,3-bis-*b-D*-maltopyranoside (LMNG, Anatrace, Maumee OH), 0.05% cholesteryl hemisuccinate (CHS), 100 mM HEPES pH 7.0, and 500 mM NaCl for 5-6 hours followed by ultracentrifugation at 200,000 x g for 30 minutes to remove solid particulates. The ratio of 20:1 (w/w) LMNG to CHS was specifically selected as an optimal mixture for NMR studies and used throughout the preparation. This ratio permitted sufficient stability of the protein over the duration of the NMR experiment while maintaining a relatively smaller micelle size enabling recording NMR data with superior resolution. The supernatant was then mixed with Co²⁺-charged affinity resin (TALON, Clontech) and 30 mM imidazole overnight at 4°C, washed with buffer 1 (25 mM HEPES pH 7.0, 500 mM NaCl, 10 mM MgCl₂, 0.1% LMNG, 0.005% CHS, 8 mM ATP, 30 mM imidazole), and twice with buffer 2 (25 mM HEPES pH 7.0, 250 mM NaCl, 0.05% LMNG, 0.0025% CHS, 5% glycerol, 30 mM imidazole and ligand) and eluted with buffer 3 (25 mM HEPES pH 7.0, 250 mM NaCl, 0.05% LMNG, 0.025% CHS, 5% glycerol, 300 mM imidazole and ligand). Samples were then exchanged into NMR buffer (20 mM HEPES pH 7.0, 75 mM NaCl, 0.025% LMNG, 0.00125% CHS and ligand) using a PD-10 desalting column. All buffers were prepared with ligand at saturating concentration, and NMR samples were concentrated to 280 μL prior to addition of 20 μL D₂O and transferring to a 5 mm Shigemi NMR tube. All samples were purified in protonated buffers

to allow proton back-exchange. The final concentrations of all samples were between 250 to 300 μM , as determined by Bradford colorimetric assay.

NMR Spectroscopy

2-dimensional [^{15}N , ^1H]-transverse relaxation-optimized spectroscopy (TROSY) (Pervushin et al., 1997) correlation spectra were measured on a Bruker Avance II 800 MHz spectrometer equipped with a 5-mm TXI-HCN probe running Topspin 3.1 (Bruker Biospin). Experiments were recorded at 307 Kelvin, and the sample temperature was calibrated using a standard commercial sample (4% methanol in methanol- d_4). Chemical shifts were referenced to an internal DSS standard and correlated with earlier studies (Eddy et al., 2018b). TROSY spectra were measured with acquisition periods of 98 ms in ^1H , 22.5 ms in ^{15}N , and a 1 s recycle delay for a total acquisition time of approximately 18 hours per experiment. NMR data were processed identically in Topspin 3.6.1 (Bruker Biospin) with the following parameters: prior to Fourier transformation, the data matrices were zero filled to 1024 (t1) x 4096 (t2) complex points and multiplied by a Gaussian window function in the direct acquisition dimension and a 75°-shifted sine bell window function in the indirect dimension.

QUANTIFICATION AND STATISTICAL ANALYSIS

All NMR spectra were analyzed and compared in Topspin 3.6.1 (Bruker Biospin) after data processing. 2D contour plots and 1D cross sections were plotted at identical levels relative to the noise floor of the spectra, unless indicated otherwise in the text.

ADDITIONAL RESOURCES

The PDB accession codes 3EML, 3REY, 3RFM, 2YDV, 3QAK, and 4UHR were referenced in this study. The UniProt accession code P29274 for human A_{2A}AR was used in this study.